



HAL
open science

C-property and Residual Distribution

Mario Ricchiuto

► **To cite this version:**

Mario Ricchiuto. C-property and Residual Distribution. [Research Report] RR-7191, INRIA. 2010. inria-00451906v2

HAL Id: inria-00451906

<https://inria.hal.science/inria-00451906v2>

Submitted on 21 Apr 2010

HAL is a multi-disciplinary open access archive for the deposit and dissemination of scientific research documents, whether they are published or not. The documents may come from teaching and research institutions in France or abroad, or from public or private research centers.

L'archive ouverte pluridisciplinaire **HAL**, est destinée au dépôt et à la diffusion de documents scientifiques de niveau recherche, publiés ou non, émanant des établissements d'enseignement et de recherche français ou étrangers, des laboratoires publics ou privés.



INSTITUT NATIONAL DE RECHERCHE EN INFORMATIQUE ET EN AUTOMATIQUE

C-property and Residual Distribution

Mario Ricchiuto

N° 7191

January 2010

Thème NUM

*R*apport
de recherche

C-property and Residual Distribution

Mario Ricchiuto*

Thème NUM — Systèmes numériques
Équipes-Projets BACCHUS

Rapport de recherche n° 7191 — January 2010 — 17 pages

Abstract: In this paper we consider the discretization the Shallow Water equations by means of Residual Distribution (RD) schemes, and review the conditions allowing the exact preservation of some exact steady solutions. These conditions are shown to be related to both the type of spatial approximation and to the quadrature used to evaluate the cell residual. Numerical examples are shown to validate the theory.

Key-words: numerical analysis, second order schemes, hyperbolic problems, residual distribution, C-property, unstructured grids

* INRIA - Bordeaux Sud-Ouest

On the C-property and generalized C-property of Residual Distribution for the Shallow Water equations

Résumé : In this paper we consider the discretization the Shallow Water equations by means of Residual Distribution (RD) schemes, and review the conditions allowing the exact preservation of some exact steady solutions. These conditions are shown to be related to both the type of spatial approximation and to the quadrature used to evaluate the cell residual. Numerical examples are shown to validate the theory.

Mots-clés : numerical analysis, second order schemes, hyperbolic problems, residual distribution, C-property, unstructured grids

Contents

| | | |
|----------|---|-----------|
| 1 | Introduction and generalities | 3 |
| 2 | Mathematical problem and notation | 3 |
| 2.1 | Particular steady solutions | 4 |
| 3 | Residual Distribution discretization | 6 |
| 3.1 | Basic properties | 7 |
| 4 | Preservation of steady solutions | 8 |
| 4.1 | Lake at rest solutions | 8 |
| 4.2 | Pseudo 1d flow solutions | 10 |
| 5 | Numerical examples | 11 |
| 6 | Final remarks | 15 |

1 Introduction and generalities

In this paper we study the application of Residual Distribution (RD) discretizations [8, 2] to the Shallow Water equations. Our objective is to determine the conditions under which a high order (RD) scheme is able to preserve exactly particular steady solutions of the problem. The discussion presented here generalizes the work of [11, 12]. Similar results have been discussed *e.g.* in [5, 10, 16, 17, 14, 15] for finite volume, WENO finite volume, and discontinuous Galerkin schemes. Here, as in [5, 10] the main focus is on two dimensional unstructured mesh approximations and, as in [14], on problems non necessarily involving trivial equilibria.

Our methodology is based on a weighted residual approach where the element integral of the equation (*viz.* the element residual) is split into nodal residuals that, once assembled, form algebraic nodal equations. The main result is that, due to the direct use the multidimensional equation to write the algebraic equations, to the continuity of the spatial approximation, and making use of an equivalence between the element integral of any quasi-linear form of the equation and the integral of the conservative form, we are able to preserve exactly steady solutions provided that : the approximation is written directly in terms of a set of steady invariants, exact integration and source term expressions are used. We will show numerical evidence that this is indeed the case, at least whenever the data of the problem are smooth.

2 Mathematical problem and notation

We consider the numerical approximation of solution to the Shallow Water Equations (SWE) :

$$\partial_t \mathbf{u} + \nabla \cdot \mathcal{F}(\mathbf{u}) + \mathcal{S}(\mathbf{u}, x, y) = 0 \quad (1)$$

where, denoting by H the water depth, by \vec{q} and \vec{v} the discharge and the local water speed such that $\vec{q} = (q_x, q_y) = H \vec{v} = H(v_x, v_y)$, \mathbf{u} is the array of

conserved quantities

$$\mathbf{u} = \begin{bmatrix} H \\ \vec{q} \end{bmatrix}$$

and \mathcal{F} is denotes the conservative fluxes

$$\mathcal{F} = [\mathcal{F}_x \ \mathcal{F}_y] \begin{bmatrix} \vec{q} \\ \vec{v} \otimes \vec{q} + g \frac{H^2}{2} \mathbf{I}_2 \end{bmatrix}$$

with \mathbf{I}_2 the 2×2 identity matrix, and g the gravity acceleration. The source term \mathcal{S} in (1) models the effects of the bathymetry $B(x, y)$ on the mean flow :

$$\mathcal{S} = gH \begin{bmatrix} 0 \\ \nabla B \end{bmatrix}$$

2.1 Particular steady solutions

By simple manipulations, we can rewrite the SWE as

$$\partial_t \mathbf{u} + \begin{bmatrix} \partial_x q_x + \partial_y q_y \\ \vec{v}(\partial_x q_x + \partial_y q_y) + H \nabla \mathcal{E} + \vec{q}^\perp (\partial_y v_x - \partial_x v_y) \end{bmatrix} = 0 \quad (2)$$

where \mathcal{E} denotes the total energy

$$\mathcal{E} = g(H + B) + \frac{\vec{v} \cdot \vec{v}}{2}$$

and \vec{q}^\perp denotes the orthogonal discharge $\vec{q}^\perp = (-q_y, q_x)$. This particular form of the equations allows to highlight a whole family of exact steady solutions involving *homoenergetic, irrotational flow, with a solenoidal discharge field*, namely

$$\begin{aligned} \mathcal{E} = g(H + B) + \frac{\vec{v} \cdot \vec{v}}{2} &= \text{constant} \\ \partial_y v_x - \partial_x v_y &= 0 \\ \partial_x q_x + \partial_y q_y &= 0 \end{aligned} \quad (3)$$

Within this family of steady states we find the following well-known steady solutions :

Lake at rest This solution is completely characterized by the initial uniform value of the state vector

$$\mathbf{v} = \begin{bmatrix} \mathcal{E} \\ \vec{q} \end{bmatrix} \quad (4)$$

This means that $\forall t \geq 0$ and $\forall (x, y)$ we have $\mathbf{v} = \mathbf{v}_0$ given by :

$$\begin{aligned} H + B = (H + B)_0 = \frac{1}{g} \mathcal{E}_0 &= \text{const} \\ q_x &= 0 \\ q_y &= 0 \end{aligned} \quad (5)$$

Clearly, the last two conditions also imply $\vec{v} = 0$, so that all of (3) are verified.

Pseudo 1d flow A generalization of the lake at rest solution can be obtained by rewriting the SWE in quasi-linear form in terms of the state vector (4). After a few manipulations one obtains :

$$\partial_t \mathbf{u} + A_{\mathbf{v}} \partial_x \mathbf{v} + B_{\mathbf{v}} \partial_y \mathbf{v} + \mathcal{S}_{\mathbf{v}}(\mathbf{v}, x, y) = 0 \quad (6)$$

with $A_{\mathbf{v}} = \partial_{\mathbf{v}} \mathcal{F}_x$ and $B_{\mathbf{v}} = \partial_{\mathbf{v}} \mathcal{F}_y$. The entries of $A_{\mathbf{v}}$ and $B_{\mathbf{v}}$ are readily obtained using the chain rule. Note however, that since \mathbf{v} depends on the bathymetry, extra terms containing the derivatives of B arise when computing these matrices, so that the expression of the source term is modified. The form of the source term is now

$$\mathcal{S}_{\mathbf{v}}(\mathbf{v}, x, y) = \frac{1}{H - \frac{\vec{u} \cdot \vec{u}}{g}} \begin{bmatrix} 0 \\ u \\ -v \end{bmatrix} \vec{q}^{\perp} \cdot \nabla B \quad (7)$$

These expressions show that a steady solution is given by $\mathbf{v} = \mathbf{v}_0 \forall t$ and $\nabla(x, y)$, provided that $\vec{q}^{\perp} \cdot \nabla B = 0$, that is provided that the bathymetry has only one dimensional variations along discharge lines. In particular, without loss of generality in the following we will refer to the pseudo 1d flow solutions as the ones for which

$$\mathbf{v} = \mathbf{v}_0 = \begin{bmatrix} \mathcal{E}_0 \\ q_0 \\ 0 \end{bmatrix} \quad \forall t \text{ and } \nabla(x, y) \quad (8)$$

and

$$B = B(x)$$

Note that these solutions basically involve one dimensional flow. Additionally, since in presence of shocks the relevant form of the SWE is the conservative form, relations (2) are no longer valid, so that the pseudo 1d solutions in general do not admit shocks. More general situations in which two different pseudo 1d flows are connected across a shock via the jump conditions are known, but will not be considered here.

Potential flow For completeness we add to the list of steady solutions the case in which the flow speed is obtained by a potential. In particular, let φ denote the scalar potential verifying

$$\Delta \varphi = 0$$

If we set $\vec{v} = (\partial_y \varphi, -\partial_x \varphi)$, one immediately sees that the second in (3) is always satisfied. Moreover, if we set $H = \varphi + H_{\infty}$, with H_{∞} a constant, the last in (3) is also automatically true. At last, the first in (3) imposes the form of the bathymetry, finally leading to the following potential solutions :

$$\begin{aligned} \Delta \varphi &= 0 \\ \vec{v} &= (\partial_y \varphi, -\partial_x \varphi) \\ H &= \varphi + H_{\infty} \\ B &= \frac{1}{g} \mathcal{E}_0 - \varphi - H_{\infty} - \frac{\|\nabla \varphi\|^2}{2g} \end{aligned} \quad (9)$$

In numerical applications one often requires the above steady solutions to be preserved exactly in some sense, so that small perturbations of these solutions can be resolved without the need of excessive mesh refinement. Schemes enjoying this property are often referred to as well balanced. The following more precise characterization can be given.

C-property A numerical scheme that preserves exactly initial solutions of the Lake at rest type (cf. equation (5)) is said to verify the *C-property*. A numerical scheme that preserves an initial lake at rest solution within an accuracy higher than that of its truncation error is said to verify the *approximate C-property*.

Generalized C-property A numerical scheme that preserves exactly initial solutions of the pseudo 1d flow type (cf. equation (8)) is said to verify the *generalized C-property*. A numerical scheme that preserves an initial pseudo 1d flow solution within an accuracy higher than that of its truncation error is said to verify the *approximate generalized C-property*.

To our knowledge, so far no scheme is able to preserve exactly potential solutions of type (9). The main difficulty lays in the need of preserving exactly the solenoidal and irrotational conditions.

3 Residual Distribution discretization

We consider discretizations of (1) based on a conservative Residual Distribution (RD) approach [7, 13]. In particular, the schemes we analyze are those discussed in [11, 12].

The basic principles of the RD discretization procedure can be summarized as follows. Let \mathcal{T}_h be an unstructured triangulation of the two dimensional spatial domain, composed of non overlapping triangles, h denoting a characteristic element size. Let T be the generic triangle of the mesh. On \mathcal{T}_h , let \mathbf{u}_h be a continuous piecewise polynomial approximation of \mathbf{u} built starting from collocated (nodal) values \mathbf{u}_i , $i \in \mathcal{T}_h$. An example of such an approximation is given by standard P^k Lagrange finite elements. In particular, we will denote by ψ_i the basis function associated to the degree of freedom \mathbf{u}_i , so that

$$\mathbf{u}_h = \sum_{i \in \mathcal{T}_h} \psi_i \mathbf{u}_i$$

On a generic element T define the *fluctuation* $\phi(\mathbf{u}_h)$

$$\phi(\mathbf{u}_h) = \oint_{\partial T} \mathcal{F}_h(\mathbf{u}_h) \cdot \hat{n} \, dl + \int_T \mathcal{S}_h(\mathbf{u}_h, x, y) \, dx \, dy \quad (10)$$

having denoted by $\mathcal{F}_h(\mathbf{u}_h)$ and $\text{source}_h(\mathbf{u}_h, x, y)$ continuous numerical approximations of the flux and of the source term, to be defined. Next consider a discretization of the time derivative. Here, we only consider the second order Crank-Nicholson operator

$$\partial_t \mathbf{u} + \nabla \cdot \mathcal{F}(u) + \mathcal{S}(\mathbf{u}, x, y) \approx \frac{\mathbf{u}^{n+1} - \mathbf{u}^n}{\Delta t} + \nabla \cdot \mathcal{F}(u^{n+1/2}) + \mathcal{S}(\mathbf{u}^{n+1/2}, x, y)$$

with Δt the time step, and $\mathbf{u}^{n+1/2} = (\mathbf{u}^{n+1} + \mathbf{u}^n)/2$. With this notation we define the *cell residual* $\Phi(\mathbf{u}_h)$

$$\Phi(\mathbf{u}_h) = \int_T \left(\frac{\mathbf{u}_h^{n+1} - \mathbf{u}_h^n}{\Delta t} + \nabla \cdot \mathcal{F}_h(u_h^{n+1/2}) + \mathcal{S}_h(\mathbf{u}_h^{n+1/2}, x, y) \right) dx dy = \int_T \frac{\mathbf{u}_h^{n+1} - \mathbf{u}_h^n}{\Delta t} dx dy + \phi(\mathbf{u}_h^{n+1/2}) \quad (11)$$

The RD discrete counterpart of (1) is obtained by splitting the cell residual to all the degrees of freedom (nodes) of element T . In particular, if $\Phi_j(\mathbf{u}_h)$ is the amount of residual distributed to $j \in T$, then

$$\sum_{j \in T} \Phi_j(\mathbf{u}_h) = \Phi(\mathbf{u}_h) \quad (12)$$

Finally, a local discrete approximation of (1) is obtained by requiring

$$\sum_{T \in \mathcal{T}_h | i \in T} \Phi_i(\mathbf{u}_h) = 0 \quad \forall i \in \mathcal{T}_h \quad (13)$$

3.1 Basic properties

The properties of scheme (12)-(13) depend on the choices made in terms of approximation (*viz.* interpolation) and distribution (*viz.* definition of Φ_j , given Φ). For a thorough discussion of these properties we refer the reader to [1, 4, 7, 11, 3, 8]. The following two properties are relevant to our discussion.

Conservation For the schemes considered here, conservation is guaranteed by the use of boundary integration of the flux in the computation of the cell residual [7]. In particular, under some continuity assumptions on the Φ_j s always verified in practice, scheme (12)-(13) verifies a Lax-Wendroff theorem, as long as the discrete approximation of the flux \mathcal{F}_h used in (10) is continuous across element edges [4].

Accuracy For continuous k -th order accurate approximations of \mathbf{u} , and of the flux and of the source, scheme (12)-(13) has a truncation error of order $\mathcal{O}(h^k)$ provided that whenever \mathbf{u}_h is the interpolant of a classical solution of (1), then (in 2d) [11, 4]

$$\Phi_j(\mathbf{u}_h) = \mathcal{O}(h^{k+1})$$

In particular, schemes for which

$$\Phi_j(\mathbf{u}_h) = \beta_j \Phi(\mathbf{u}_h)$$

with β_j a *uniformly bounded* distribution matrix have a $\mathcal{O}(h^k)$ truncation error [11, 4].

In all the numerical applications shown in the paper, we will make use of the stabilized limited Lax-Friedrich's RD scheme presented in detail in [12]. Even though the analysis presented in this paper remains valid in the general case of P^k interpolation, we will focus on a P^1 approximation in space, using the Crank-Nicholson scheme in time.

4 Preservation of steady solutions

The constraints given so far on the RD discretization allow for the construction of high order conservative schemes. The question we want to answer now is how to ensure the satisfaction of the C-property and/or of its generalized variant. In particular, two degrees of freedom are left : the choice of the spatial approximation of the unknown \mathbf{u} , and that of flux and source needed for the evaluation of the fluctuation ϕ .

To begin with, let us have a look at the discrete equations (13). These define a system of nonlinear algebraic equations for the nodal values \mathbf{u}_i . The solution of such system is obtained by means of some iterative procedure such as a standard Newton algorithm, or as an explicit fixed point algorithm as the one employed in [12]. As an example, we can consider the case of a dumped Newton procedure. If we set $\mathbf{w} = \mathbf{u}^{n+1}$, the dumped Newton loop writes

$$\sum_{T \in \mathcal{T}_h} \sum_{i \in T} \sum_{j \in T} \left(\frac{\delta_{ij}}{\omega_i} + (\partial_{\mathbf{u}_j} \Phi_i)^k \right) (\mathbf{w}_j^{k+1} - \mathbf{w}_j^k) = - \sum_{T \in \mathcal{T}_h} \Phi_i^k,$$

where ω_i is the dumping parameter. When initializing the loop with $\mathbf{w}^0 = \mathbf{u}^n$ we have on the right hand side, for a high order RD

$$\Phi_i^0 = \beta_i \Phi^0 = \beta_i \left(\int_T \frac{\mathbf{w}_h^0 - \mathbf{u}_h^n}{\Delta t} dx dy + \phi \left(\frac{\mathbf{w}_h^0 + \mathbf{u}_h^n}{2} \right) \right) = \beta_i \phi(\mathbf{u}_h^n),$$

so that we end with

$$\sum_{T \in \mathcal{T}_h} \sum_{i \in T} \sum_{j \in T} \left(\frac{\delta_{ij}}{\omega_i} + (\partial_{\mathbf{u}_j} \Phi_i)^k \right) (\mathbf{w}_j^1 - \mathbf{u}_j^n) = - \sum_{T \in \mathcal{T}_h} \beta_i \phi_i(\mathbf{u}_h^n).$$

Clearly, if $\phi(\mathbf{u}^n) = 0 \forall T$, the Newton algorithm converges in one iteration to the solution $\mathbf{w} = \mathbf{u}^{n+1} = \mathbf{u}^n$. Hence, our objective is to select the spatial approximation, and the continuous approximation of the flux and of the source, such that

$$\phi(\mathbf{u}_h) = \oint_{\partial T} \mathcal{F}_h(\mathbf{u}_h) \cdot \hat{n} dl + \int_T \mathcal{S}_h(\mathbf{u}_h, x, y) dx dy = 0.$$

4.1 Lake at rest solutions

The preservation of the lake at rest solution is easily achieved in the RD context. Early results showing the potential of the approach can be found in [6]. The approach discussed here is a generalization of the construction proposed in the last reference. The idea is to exploit the fact that we have a set of steady invariants \mathbf{v} . We would like to express the discrete equations in terms of differentials of \mathbf{v} . In our case, this means that the approximation should be

$$\mathbf{u}_h = \mathbf{u}(\mathbf{v}_h) \quad \text{with} \quad \mathbf{v}_h = \sum_{i \in \mathcal{T}_h} \psi_i \begin{bmatrix} g(H_i + B_i) \\ \vec{q}_i \end{bmatrix}.$$

On the lake at rest solution we have $\mathbf{v}_h = \mathbf{v}_0$. If we now look at the fluctuation ϕ we have :

$$\phi = \oint_{\partial T} \begin{bmatrix} 1 \\ \vec{u}_h \end{bmatrix} \vec{q}_h \cdot \hat{n} dl + \oint_{\partial T} \begin{bmatrix} 0 \\ g \frac{H_h^2}{2} \end{bmatrix} \hat{n} dl + \int_T \begin{bmatrix} 0 \\ g H_h \nabla B_h \end{bmatrix} dx dy = \oint_{\partial T} \begin{bmatrix} 0 \\ g \frac{H_h^2}{2} \end{bmatrix} \hat{n} dl + \int_T \begin{bmatrix} 0 \\ g H_h \nabla B_h \end{bmatrix} dx dy .$$

At this point we still have to choose how to represent the bathymetry. Note that, independently on this choice, for exact integration we can apply Gauss' theorem to get

$$\phi = \int_T \begin{bmatrix} 0 \\ H_h \nabla \mathcal{E}_h \end{bmatrix} dx dy = \int_T \begin{bmatrix} 0 \\ H_h \nabla \mathcal{E}_0 \end{bmatrix} dx dy = 0 ,$$

which shows that

Proposition 4.1 (C-property - Exact integration). *When using exact integration, a high order RD scheme verifies the C-property, provided that the fluctuation is evaluated using the approximation written in terms of the steady invariants $[g(H+B) \vec{q}]^t$.*

Exact integration is of course never used in practice. A logical choice is to assume for the bathymetry the same variation used for the invariants, namely $B_h = \sum_{i \in \mathcal{T}_h} \psi_i B_i$. In this case we recover the constructions of [6] and [11, 12], which are very similar to the hydrostatic reconstruction used *e.g.* in [5]. In particular, we have $H_h = \mathcal{E}_h/g - B_h$ which belongs now to the same polynomial space used for the approximation. In this case, we can indeed use exact integration with respect to this polynomial variation obtaining, as before, the exact preservation of the lake at rest state.

Proposition 4.2 (C-property - Same approximation for depth and bathymetry). *When using the same polynomial approximation for H_h and B_h and exact integration with respect to this assumption, a high order RD scheme verifies the C-property.*

The last possibility is that of using for B its exact expression, while evaluating ϕ with approximate integration. In this case, provided that B is smooth enough, the accuracy obtained will depend on the quadrature formula used in practice. An estimate of the asymptotic behavior of the error can be obtained by studying the explicit fixed point resolution technique used in [12]. In this approach, the Newton loop is replaced by the following update

$$\mathbf{w}_i^{k+1} = \mathbf{w}_i^k - \omega_i \sum_{T \in \mathcal{T}_h | i \in T} (\beta_i \Phi)^k ,$$

with ω_i a relaxation parameter, that can be easily shown to be bounded by $\mathcal{O}(h^{-1})$ for stability reasons[12]. In the following we assume $\omega_i = \mathcal{O}(h^{-1})$. Suppose now that the bathymetry has a smooth variation, and that we evaluate the line integrals in the fluctuation with formulas exact for polynomials of degree p_l , and the surface integrals with formulas exact for polynomials of degree p_s .

On the lake at rest solution we have

$$\begin{aligned} \phi &= \oint_{\partial T} \begin{bmatrix} 0 \\ g \frac{H_h^2}{2} \end{bmatrix} \hat{n} dl + \int_T \begin{bmatrix} 0 \\ g H_h \nabla B_h \end{bmatrix} dx dy \\ &= \int_T \begin{bmatrix} 0 \\ H_h \nabla \mathcal{E}_0 \end{bmatrix} dx dy + \max(\epsilon_{p_l}, \epsilon_{p_s}) = \max(\epsilon_{p_l}, \epsilon_{p_s}) = \max(\mathcal{O}(h^{p_l+2}), \mathcal{O}(h^{p_s+3})) \end{aligned}$$

where the last estimates are readily obtained by *e.g.* bounding truncated Taylor developments of the integrand.

The first explicit fixed point iteration will give

$$\mathbf{w}_i^1 = \mathbf{u}_i^n + \mathcal{O}(h^{-1})\mathcal{O}(\phi(\mathbf{v}_h^n)) = \mathbf{u}_i^n + \max(\mathcal{O}(h^{p_l+1}), \mathcal{O}(h^{p_s+2})).$$

Starting from the second iteration we have to take into account the time variation of the solution. Neglecting variations on the asymptotic order of ϕ , we can write

$$\begin{aligned} \Phi_i &= \beta_i \Phi = \beta_i \left(\mathcal{O}\left(\frac{|T|}{\Delta t}\right) \mathcal{O}(\mathbf{w}^1 - \mathbf{u}^n) + \mathcal{O}(\phi) \right) = \\ &= \beta_i (\mathcal{O}(h) \max(\mathcal{O}(h^{p_l+1}), \mathcal{O}(h^{p_s+2})) + \max(\mathcal{O}(h^{p_l+2}), \mathcal{O}(h^{p_s+3}))) , \\ &= \max(\mathcal{O}(h^{p_l+2}), \mathcal{O}(h^{p_s+3})) \end{aligned}$$

which easily leads to the result that for the k -th iterate we have

$$\mathbf{w}_i^{k+1} = \mathbf{w}_i^k + \max(\mathcal{O}(h^{p_l+1}), \mathcal{O}(h^{p_s+2})) = \dots = \mathbf{u}_i^n + \max(\mathcal{O}(h^{p_l+1}), \mathcal{O}(h^{p_s+2})). \quad (14)$$

This shows that

Proposition 4.3 (Approximate C-property). *When using approximate quadrature and the exact variation of the bathymetry, high order RD verify the approximate C-property, provided that the bathymetry variations are smooth enough. A coarse estimate of the error on the solution is $\epsilon = \max(\mathcal{O}(h^{p_l+1}), \mathcal{O}(h^{p_s+2}))$ if the line quadrature formulas used are exact for polynomials of degree p_l and the surface quadrature formulas are exact for polynomials of degree p_s .*

4.2 Pseudo 1d flow solutions

In the case of pseudo 1d flow solutions, we are unfortunately not able to provide a simple and general strategy using the same polynomial for the depth and the bathymetry. Things are much easier in a purely one dimensional context, in which our RD approach has very close similarities to the regular/singular residual decomposition approach discussed in [14, ?]. When looking at the problem from a multidimensional perspective, which is a must on unstructured grids, we can however repeat the asymptotic analysis discussed for the lake at rest state.

In particular, when evaluating the fluctuation we set $\mathbf{u}_h = \mathbf{u}(\mathbf{v}_h)$, where \mathbf{v} is now given by (8), with \mathcal{E} as in (3). Also, we set $\mathcal{F}_h = \mathcal{F}(\mathbf{v}_h)$, and $\mathcal{S}_h = \mathcal{S}(\mathbf{v}_h, x, y)$, and use the exact expression of the bathymetry. Since all the quantities are continuous and differentiable within an element (provided

that the bathymetry is), when using exact integration we can use Gauss' theorem and chain rule differentiation to get (cf. section §2.1, equations (6) and (7))

$$\phi(\mathbf{v}_h) = \int_T (\partial_t \mathbf{u} + A_{\mathbf{v}}(\mathbf{u}_h) \partial_x \mathbf{v}_h + B_{\mathbf{v}}(\mathbf{v}_h) \partial_y \mathbf{v}_h + \mathcal{S}_{\mathbf{v}}(\mathbf{v}_h, x, y)) dx dy = \int_T \frac{1}{H_h - \frac{\vec{u}_h \cdot \vec{u}_h}{g}} \begin{bmatrix} 0 \\ u_h \\ -v_h \end{bmatrix} \vec{q}_h^\perp \cdot \nabla B dx dy.$$

Since, by hypothesis we are using the exact representation of the bathymetry, we will have (cf. equation (8)) $\nabla B = (\partial_x B, 0)$. Since $\vec{q}_h^\perp = (0, q_{xh})$, the source term vanishes, and so does the fluctuation. Hence

Proposition 4.4 (Generalized C-property - Exact integration). *When using exact integration, high order RD verify the C-property, provided that the fluctuation is evaluated using the exact bathymetry and the approximation written in terms of the steady invariants $[\mathcal{E} \ \vec{q}]^t$.*

As in the case of the lake at rest solution, exact integration is in practice replaced by numerical quadrature. Also for the pseudo 1d solutions, if the regularity of the bathymetry is high enough, we can estimate the quadrature error, and the perturbation introduced in the numerical solution. The analysis is identical to the one performed for the lake at rest and again leads to the final estimate (14).

Proposition 4.5 (Approximate generalized C-property). *When using approximate quadrature and the exact variation of the bathymetry, high order RD verify the approximate generalized C-property, provided that the bathymetry variations are smooth enough. A coarse estimate of the error on the solution is $\epsilon = \max(\mathcal{O}(h^{p_l+1}), \mathcal{O}(h^{p_s+2}))$ if the line quadrature formulas used integrate exactly polynomials of degree p_l and the surface quadrature formulas are exact for polynomials of degree p_s .*

5 Numerical examples

This section provides a numerical verification of the theory discussed. Results showing the respect of the C-property when using the same approximation for the depth and for the bathymetry (cf. proposition 4.2) have been published already in [11, 12]. We refer to these references for a thorough numerical assessment of this approach.

Here we are more interested in the numerical verification of propositions 4.3 and 4.5. In particular, our main interest is the verification of the estimate (14). To do this we will consider a simple test case involving a pseudo-one dimensional variation of the bathymetry. All the test cases involve the spatial domain $[0, 25]^2$, over which we impose three different variations of the bathymetry :

Case T1 In this case we take $B = B(x)$, with given by

$$B(x) = \begin{cases} 0.2 - 0.05(x - 10)^2 & \text{if } x \in [8, 12] \\ 0 & \text{otherwise} \end{cases}.$$

Case T2 In this case we take $B = B(x)$ given by

$$B(x) = \begin{cases} 0.2 \sin(0.25\pi(x-8))^4 & \text{if } x \in [8, 12] \\ 0 & \text{otherwise} \end{cases} .$$

Case T3 In this case we take $B = B(x)$ given by

$$B(x) = \begin{cases} 0.2 \sin(0.25\pi(x-8))^6 & \text{if } x \in [8, 12] \\ 0 & \text{otherwise} \end{cases} .$$

The objective is to have bathymetries with different regularity in order to be able to test the influence of this parameter on the validity of (14).

All the computations have been run on unstructured grids as the one reported in figure 1. The unstructured nature of the meshes introduces a multi-dimensional character in the tests, since no preferential direction is present. In particular, all the grid refinement studies have been performed by conformally refining the mesh of figure 1. Three levels of refinement have been considered. The coarsest mesh size is $h \approx 25/40$.

We have considered three quadrature strategies :

Strategy Q1 We use 2 line quadrature points corresponding to the trapezium rule, and 1 surface quadrature point, corresponding to mid-point quadrature. Both formulas integrate exactly polynomials of degree 1, hence the expected accuracy, according to (14) is

$$\epsilon = \mathcal{O}(\max(h^2, h^3)) = \mathcal{O}(h^2) .$$

Strategy Q2 We use a standard 2 points Gaussian line quadrature formula, and a 6 points surface quadrature formula. The Gaussian formula integrates exactly polynomials of degree 3, while the surface formula integrates exactly polynomials of degree 4. Hence the expected accuracy, according to (14) is

$$\epsilon = \mathcal{O}(\max(h^4, h^6)) = \mathcal{O}(h^4) .$$

Strategy Q3 We use a standard 3 points Gaussian line quadrature formula, and a 6 points surface quadrature formula. The Gaussian formula integrates exactly polynomials of degree 5, while the surface formula integrates exactly polynomials of degree 4. Hence the expected accuracy, according to (14) is

$$\epsilon = \mathcal{O}(\max(h^6, h^6)) = \mathcal{O}(h^6) .$$

The 6 point surface quadrature formula has been taken from [9].

We consider both an initial lake at rest state, and a pseudo 1d flow state. In both cases the initial value for the total energy is taken as $\mathcal{E}_0 = 22.06605$. In the lake at rest solution we obviously set $q_0 = 0$, while for the pseudo 1d solution we take $q_0 = 4.42$.

Time dependent computations have been run with the LLFs scheme described in detail in [12]. In particular, we set the initial solution to the exact steady one and let the scheme compute an unsteady solution until the final

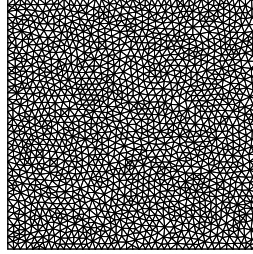


Figure 1: Unstructured triangulation used in the numerical tests

time $t_f = 0.1$. We then compute the error on the total energy between the final solution and the exact/initial one.

The results for the lake at rest case are reported on figures 2, 3, and 4. In the figures we plot the grid convergence of the error for the cases T1, T2, and T3, comparing the three quadrature strategies with the prediction of (14).

From figure 2 we see that all the strategies fail to reach even the level of truncation error of the scheme, which is second order. This is definitely due to the lack of regularity of the bathymetry. Indeed, in the case T1, the function $B(x)$ is only continuous, hence all formulas basically give first order of accuracy. The slope observed is indeed between 1 and 2, as shown in the picture.

More interesting is the result of figure 3. In this case, the slopes observed are in perfect agreement with (14) for the strategies Q1 and Q2. For the quadrature Q3 we only observe fourth order of convergence, instead of the sixth order predicted by (14). However, in this case the bathymetry only has three continuous derivatives, which explains why we cannot obtain more than fourth order of accuracy, which is indeed what we get with the strategy Q3.

Finally, the results for the T3 test case, shown in figure 4, confirm the validity of (14). In this case, the bathymetry has enough continuous derivatives to achieve the theoretical sixth order of convergence when using the Q3 strategy, confirming the validity of proposition 4.3.

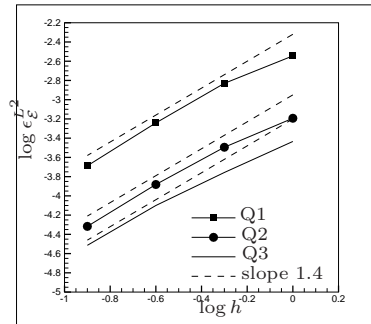


Figure 2: Grid convergence for the case T1, lake at rest with $\mathcal{E}_0 = 22.06605$

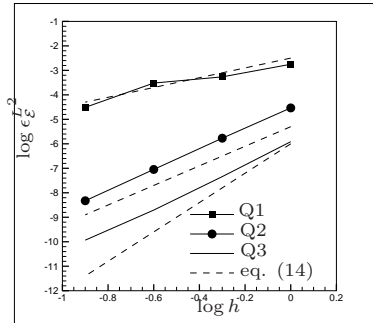


Figure 3: Grid convergence for the case T2, lake at rest with $\mathcal{E}_0 = 22.06605$. The dashed line next to each convergence curve represents the corresponding slope as predicted by equation (14).

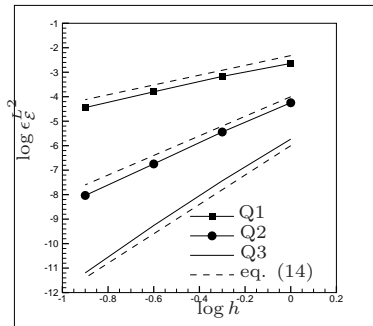


Figure 4: Grid convergence for the case T3, lake at rest with $\mathcal{E}_0 = 22.06605$. The dashed line next to each convergence curve represents the corresponding slope as predicted by equation (14).

The results obtained for the pseudo 1d flow problem are identical in nature to the ones discussed for the lake at rest state. The grid convergence plots comparing the different quadrature strategies are reported in figures 5, 6, and 7.

As before, the bathymetry in T1 is only continuous, and the accuracy observed is between one and two, as we can see on figure 5. As we can see on figure 6, the scheme does better in case T2, in which we can get both the second and fourth orders of accuracy predicted by (14) for the quadrature strategies Q1 and Q2. In the case of quadrature Q3 we get again a fourth order slope, due to the lack of regularity of $B(x)$. The fact that for the same bathymetry we get the same behavior in the lake at rest and in the pseudo 1d flow case is encouraging. It confirms our theoretical analysis that the error is only related to quadrature, hence to the regularity of the data.

At last, we can see on figure 7 that also for the pseudo 1d flow solution when the data is regular enough, equation (14) predicts correctly the asymptotic error, thus confirming the validity of proposition 4.5.

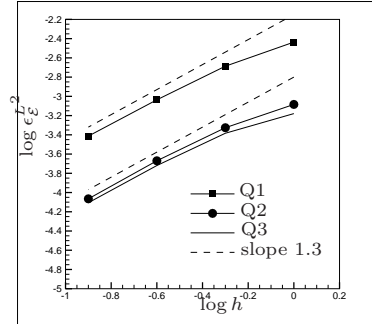


Figure 5: Grid convergence for the case T1, pseudo-1d flow with $q_0 = 4.42$ and $\mathcal{E}_0 = 22.06605$

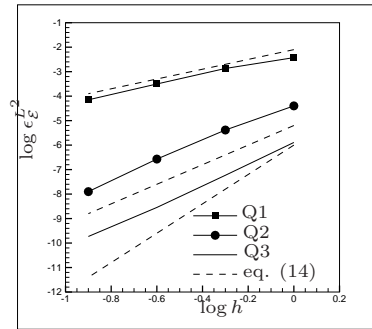


Figure 6: Grid convergence for the case T2, pseudo-1d flow with $q_0 = 4.42$ and $\mathcal{E}_0 = 22.06605$. The dashed line next to each convergence curve represents the corresponding slope as predicted by equation (14).

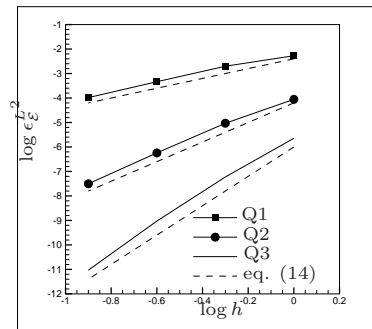


Figure 7: Grid convergence for the case T3, pseudo-1d flow with $q_0 = 4.42$ and $\mathcal{E}_0 = 22.06605$. The dashed line next to each convergence curve represents the corresponding slope as predicted by equation (14).

6 Final remarks

In this paper we have analyzed the satisfaction of the C-property and of the generalized C-property when using high order residual distribution schemes to

discretize the shallow Water equations. We have provided simple arguments to prove that provided that the approximation is written in the correct set of variables, one can obtain at least the approximate version of these properties on arbitrary triangulations, provided that the exact bathymetry is used when discretizing the formulas. An estimate of the asymptotic error has been given and confirmed by numerical computations.

From the practical point of view the need of using the exact data is a drawback, since these data are often not available in the form of an equation. Moreover the dependence of the accuracy on the regularity or the bathymetry is also a limitation, the variation of the bed slope being often quite irregular.

However, we judge our exercise interesting in the sense that it points out in 2d the need of a truly multidimensional approach, as well as the need of more information. In particular, in the case of the pseudo 1d flow, the form of the source term in (7) suggests that the variations of the bathymetry in the cross stream direction are important and, hence, a truly multidimensional treatment is needed if one wants to resolve better these non-trivial equilibria.

Other approaches in which the bathymetry is reconstructed with polynomials of higher degree than the solution, or in which one adopts a local stream-aligned reference frame to decompose different components of ∇B are of course also possible. The real challenge is also to be able to handle more complex 2d solutions such as the potential solution (9). All these topics will be explored in the future.

Acknowledgements

The author would like to express his gratitude to the organizers of the conference “Numerical approximations of hyperbolic systems with source terms and applications” for their warm welcome. The discussions with Remi Abgrall, Andreas Bollermann, Smadar Karni and Sebastian Noelle have been very helpful in the development of this work.

References

- [1] R. Abgrall. Toward the ultimate conservative scheme : Following the quest. *J. Comput. Phys*, 167(2):277–315, 2001.
- [2] R. Abgrall. Residual distribution schemes: Current status and future trends. *Computers and Fluids*, 35(7):641–669, 2006.
- [3] R. Abgrall, A. Larat, M. Ricchiuto, and C. Tavé. Simplified stabilisation procedures for residual distribution schemes. *Computer and Fluids*, 38(7):1314–1323, 2009.
- [4] R. Abgrall and P.L. Roe. High order fluctuation schemes on triangular meshes. *J. Sci. Comput.*, 19(3):3–36, 2003.
- [5] E. Audusse and M.-O. Bristeau. A well-balanced positivity preserving second order scheme for shallow water flows on unstructured meshes. *J. Comput. Phys.*, 206(1):311–333, 2005.

-
- [6] P. Brufau and P. García-Navarro. Unsteady free surface flow simulation over complex topography with a multidimensional upwind technique. *J. Comput. Phys.*, 186(2):503–526, 2003.
- [7] Á. Csík, M. Ricchiuto, and H. Deconinck. A conservative formulation of the multidimensional upwind residual distribution schemes for general non-linear conservation laws. *J. Comput. Phys.*, 179(2):286–312, 2002.
- [8] H. Deconinck and M. Ricchiuto. Residual distribution schemes: foundation and analysis. In E. Stein, R. de Borst, and T.J.R. Hughes, editors, *Encyclopedia of Computational Mechanics*. John Wiley & Sons, Ltd., 2007. DOI: 10.1002/0470091355.ecm054.
- [9] D.A. Dunavant. High degree efficient symmetrical gaussian quadrature rules for the triangle. *Int. J. Numer. Methods in Engrg.*, 21:1129–1148, 1985.
- [10] A. Kurganov and G. Petrova. A Second-Order Well-Balanced Positivity Preserving Central-Upwind Scheme for the Saint-Venant System. *Comm.Math.Sci.*, 5(1):133–160, 2007.
- [11] M. Ricchiuto, R. Abgrall, and H. Deconinck. Application of conservative residual distribution schemes to the solution of the shallow water equations on unstructured meshes. *J. Comput. Phys.*, 222:287–331, 2007.
- [12] M. Ricchiuto and A. Bollermann. Stabilized residual distribution for shallow water simulations. *J. Comput. Phys.*, 228(4):1071–1115, 2009.
- [13] M. Ricchiuto, Á. Csík, and H. Deconinck. Residual distribution for general time dependent conservation laws. *J. Comput. Phys.*, 209(1):249–289, 2005.
- [14] Y. Xing S. Noelle and C.-W. Shu. High-order well-balanced finite volume WENO schemes for shallow water equations with moving water. *J. Comput. Phys.*, 226(1):29–58, 2007.
- [15] H.C. Yee W. Wang, C.-W. Shu and B. Sjögren. High-order well-balanced schemes and applications to non-equilibrium flow. *J. Comput. Phys.*, 228(1):6682–6702, 2009.
- [16] Y. Xing and C.-W. Shu. High-order finite difference WENO schemes with the exact conservation property for the shallow-water equations. *J. Comput. Phys.*, 208(1):206–227, 2005.
- [17] Y. Xing and C.-W. Shu. High-order well-balanced finite volume WENO schemes and discontinuous Galerkin methods for a class of hyperbolic systems with source terms. *J. Comput. Phys.*, 214(2):567–598, 2006.



Centre de recherche INRIA Bordeaux – Sud Ouest
Domaine Universitaire - 351, cours de la Libération - 33405 Talence Cedex (France)

Centre de recherche INRIA Grenoble – Rhône-Alpes : 655, avenue de l'Europe - 38334 Montbonnot Saint-Ismier
Centre de recherche INRIA Lille – Nord Europe : Parc Scientifique de la Haute Borne - 40, avenue Halley - 59650 Villeneuve d'Ascq
Centre de recherche INRIA Nancy – Grand Est : LORIA, Technopôle de Nancy-Brabois - Campus scientifique
615, rue du Jardin Botanique - BP 101 - 54602 Villers-lès-Nancy Cedex
Centre de recherche INRIA Paris – Rocquencourt : Domaine de Voluceau - Rocquencourt - BP 105 - 78153 Le Chesnay Cedex
Centre de recherche INRIA Rennes – Bretagne Atlantique : IRISA, Campus universitaire de Beaulieu - 35042 Rennes Cedex
Centre de recherche INRIA Saclay – Île-de-France : Parc Orsay Université - ZAC des Vignes : 4, rue Jacques Monod - 91893 Orsay Cedex
Centre de recherche INRIA Sophia Antipolis – Méditerranée : 2004, route des Lucioles - BP 93 - 06902 Sophia Antipolis Cedex

Éditeur
INRIA - Domaine de Voluceau - Rocquencourt, BP 105 - 78153 Le Chesnay Cedex (France)
<http://www.inria.fr>
ISSN 0249-6399